Sequence Length Distributions (Microstructure) of Regioregular Poly(3-alkylthiophene)s and Related Conjugated Polymers and Their Use in Simulating $\pi-\pi^*$ Absorption Peak Profiles

M. David Curtis

Department of Chemistry, and The Macromolecular Science and Engineering Center, The University of Michigan, Ann Arbor, Michigan 48109-1055

Received June 20, 2001; Revised Manuscript Received August 17, 2001

ABSTRACT: The head−tail (HT) sequence length distributions (SLDs) of poly(3-alkylthiophenes) (P3ATs) and related polymers may be obtained from the H NMR spectra. The results show that the regioregular polymers, i.e., those with the highest HT content, have broader SLDs than the less regular polymers. The SLD may be used to simulate the characteristic profiles of the $\pi-\pi^*$ absorption peaks of **P3AT**s and related polymers.

Introduction

The solid-state morphology of conjugated polymers plays a major role in bulk transport properties of energy (excitons) or charge (conductivity).[1−6] Both exciton migration and carrier mobility are strongly modulated by π-stacking of the conjugated chains. By π-stacking, we mean the cofacial packing of the polymer main chains in the solid state. Unsubstituted conjugated polymers and oligomers, e.g., sexithiophene, tend to crystallize in the "herringbone" or "parquet" pattern wherein the edge ($\delta+$) of one chain is more or less pointed at the face ($\delta-$) of a neighboring chain (Figure 1a).[7] If the polymer or oligomer chains were substituted with alkyl side groups, then a herringbone-type packing would produce a nanoporous structure (Figure 1b). Since the energy tends to be minimized with increasing packing density, porous structures are metastable and tend to collapse to more highly packed structures, e.g., the lamellar structure shown in Figure 1c. The lamellar structure is adopted by a variety of regioregular polymers, including poly(3-alkylthiophene)s (**P3AT**s),[8] poly(3-alkyfuran)s (**P3AF**s),[9] poly(4,4′-dialkyl-2,2′-bithiazole)s (**PABTz**'s),[10] and poly(4,4′-dialkyl-2,2′-bisoxazole)s (**PABO**s).[11]

The molecular packing shown in Figure 1c is maximal, and the alkyl side chains possess translational symmetry along the chain axis; i.e., the polymers must be "regioregular". Two types of regioregularity are currently known: the −(HT−HT)− (head−tail) and −(HH−TT)− (head−head, tail−tail) types. The former is exemplified by regioregular **P3AT**s and **P3AF**s and the latter by **PABTz**'s and **PABO**s (Figure 2).

The synthesis of the HH−TT regioregular polymers may use a variety of coupling reactions because the "monomers", a bithiophene, bithiazole, or bisoxazole, have end-for-end symmetry (m or C_2, depending on conformation). In contrast, the HT−HT regioregular polymers are made from an asymmetric monomer and require a regiospecific coupling reaction, e.g., the McCullough or Rieke methods.[4,5] These coupling reactions are not perfect, and HT contents of 90−98% are obtained. In favorable circumstances, oxidative coupling can also produce polymers with high percentages of HT couplings.[12] Other polymerization reactions, e.g., Ni(COD)$_2$-mediated coupling of 2,5-dibromothiophenes,

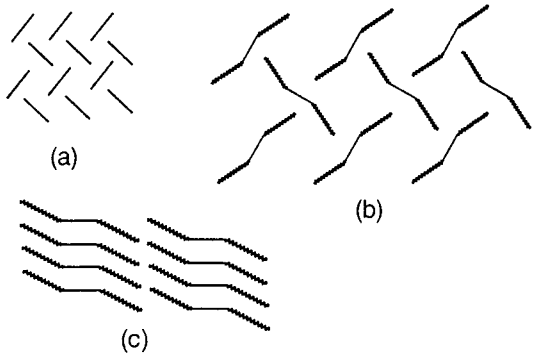

Figure 1. Views down the chain axis of (a) the herringbone structure of unsubstituted conjugated polymers, e.g., PT, (b) a hypothetical herringbone pattern of a **P3AT**, and (c) the lamellar structure of **P3AT** and related polymers.

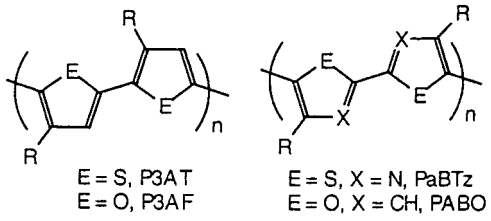

Figure 2. Structures of HT-P3AT, HT-P3AF, HH,TT-PABTz, and HH,TT-PABO.

-furans, etc., typically give HT contents around 70−75%. Regiorandom (HT = 50%) polymers are obtained by Pd-catalyzed coupling of 2-bromo-5-metallo monomers.[5] Regioregularity is manifested in a variety of important physicochemical properties, e.g., conductivity of doped samples,[4,5] FET carrier mobilities,[1f] photoluminescence efficiency,[2] UV−vis spectra,[1a] crystallinity, etc.

The HT content only partially describes the regiochemistry. The sequence length distribution is also important, as shown by the following example. Let a monomer unit with the alkyl group pointing to the left be represented by the number "0", and let a unit with the alkyl group to the right be represented by a "1".

Then the sequence, **A**, 00000000001111111111 has 10 each "left" and "right" monomer units, nine each 00 and 11 diads, and one 01 diad. The 00 and 11 diads represent HT couplings, and the 01 diad is a TT coupling

10.1021/ma011053j CCC: $20.00
Published on Web 09/29/2001

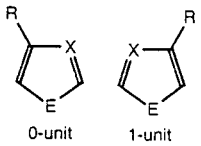

(a 10 diad is HH). Thus, 18 out of the 19 couplings are HT (95%). The sequence, **B**, 00000000010100000000 has 18 "0" units and two "1" units, 15 HT couplings (83%), two 01 diads (TT coupling), and two 10 diads (HH coupling). Despite its lower HT content, the second sequence (**B**) might disrupt crystallinity less than the first. The first sequence resembles a diblock polymer in which the two blocks are incompatible in the sense that right-pointing alkyl groups do not fit into a "left-pointing" lattice. Note: an end-for-end rotation of the polymer chain interconverts 0 and 1 units, so that "left" and "right" have no intrinsic meaning, but a given crystalline domain will be either all left or all right. This is because the π-stacked, lamellar morphology is driven by the crystallization of the side chains, which adopt the fully extended (all-trans) conformation and pack in parallel sheets (Figure 3). Thus, sequence distributions will be important in setting crystal domain size, π-stacking distances, etc., and, therefore, all the physical properties that depend on these parameters.

This paper presents the results of an analysis of the sequence length distributions in **P3AT**s and related polymers.[13] The problem is identical to the statistical treatment of the microstructure of vinyl polymers,[14−16] but the formalism has not been applied heretofore to HT sequence distributions in conjugated polymers.

NMR Spectra and Sequence Length Distributions (SLDs)

The first-order Markovian treatment of vinyl polymer microstructure gives the result

$$P_0 = p_{10}/(p_{10} + p_{01}), \quad P_0 + P_1 = 1 \tag{1}$$

where P_0 and P_1 are the unconditional probabilities of the occurrence of either a "0"- or a "1"-monomer, and "0" and "1" refer to the different monomer unit chiralities. The quantities, p_{ij}, are the conditional or "transition" probabilities of an "*i*"-unit adding a "*j*"-unit, and

$$p_{00} + p_{01} = p_{11} + p_{10} = 1 \tag{2}$$

In the context of **P3AT**s and related polymers, the same formalism may be used with a "0" monomer unit denoting a ring with the alkyl group pointing to the left and a "1" unit a ring with the alkyl group to the right. Since an end-over-end rotation of the polymer chain interconverts 0- and 1-monomer units, it follows that the probability of the occurrence of 0- and 1-units must be identical, i.e., $P_0 = P_1 = {}^1/_2$ and $p_{01} = p_{10}$ and $p_{11} = p_{00}$. Since the 00- and 11-diads represent HT (head-to-tail) coupling, we set

$$p_{HT} = p_m = p_{00}, \quad p_{HH} = p_r = p_{01}, \quad p_m + p_r = 1 \tag{3}$$

Thus, the Bovey model is appropriate for describing the microstructure of **P3AT**s and related polymers. In the following discussion, the Bovey p_m and p_r nomenclature will be used to emphasize the similarity of the side chain microstructure of **P3AT**s to that of vinyl polymers, but it must be kept in mind that "m" and "r" no longer denote "meso" and "racemo", but HT and HH, respectively. With these definitions and constraints, the fractional molar concentrations of any *n*-ad, ($m_x r_y$), is simply $p_m{}^x\ p_r{}^y$; i.e., the fractional concentrations are Bernoulian *in the Bovey basis set* (sometimes referred to as "skewed Bernoulian").

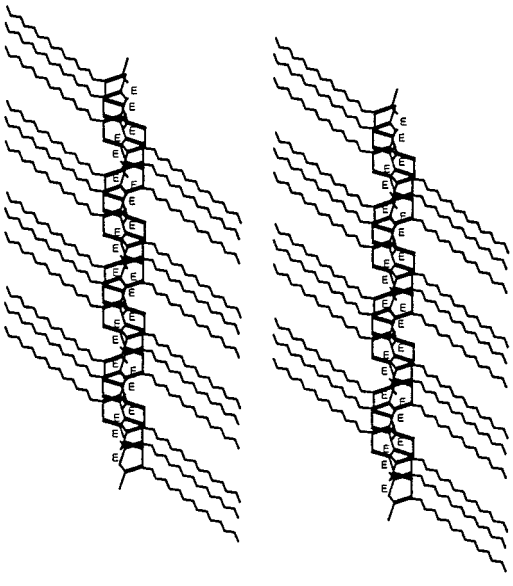

Figure 3. Side chain crystallization in HT-regioregular P3AT ("top" view of lamellar structure).

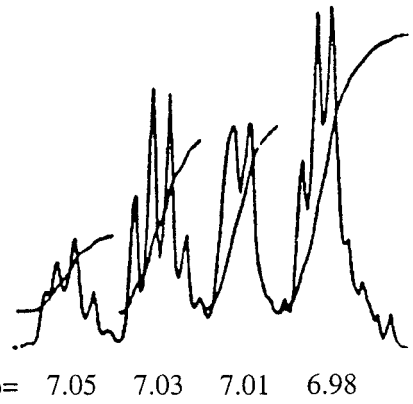

Figure 4. High-resolution, 500 MHz ^{1}H NMR spectrum of the ring protons in a 65% HT-P3BT.

The ^{1}H NMR resonance of the α-CH_2 groups on the alkyl side chains of **P3AT**s and related polymers is sensitive to the diad structure. The α-CH_2 resonance of an HT diad typically appears slightly downfield from that of the HH diad. Thus, the relative concentration (m) of the HT or m-diad, and, hence, the value of p_m is given by the fractional area of the HT α-CH_2 resonance:

$$(m) = p_m = A_{HT}/(A_{HT} + A_{HH}) \tag{4}$$

The ring protons of **P3AT**s are known to be sensitive to the triad level. Figure 4 shows the 500 MHz ^{1}H NMR spectrum of the ring proton resonances of a poly(3-butylthiophene) prepared by a Pd(0)-catalyzed coupling of 2,5-bis(chloromercurio)-3-butylthiophene.[17] Figure 4 shows four sets of peaks that have been assigned to the rr (010 + 101), rm (100 + 110), mr (001 + 011), and mm (000 + 111) triads (from high field to low).[18,19] Figure 4 also shows, possibly for the first time, that the ring protons are at least partially sensitive to the microstructure out to the pentad level as evidenced by the additional splitting of each of the main triad peaks.

As determined from integration of the α-CH_2 resonances, this particular P3BT has 65% HT diad content so that $p_m = 0.65$ and $p_r = 0.35$. Therefore, the relative concentrations of the rr, rm, mr, and mm triads are $(0.35)^2$, (0.35)(0.65), and $(0.65)^2 = 0.12$, 0.23, 0.23, and 0.42, in excellent agreement with the measured relative peak areas of 0.11, 0.24, 0.26, and 0.39.

If the further splitting of the peaks shown in Figure 4 is due to pentad structure, then each of the triad peaks should be split into four peaks corresponding to the pentads, r(xy)r, r(xy)m, m(xy)r, and m(xy)m (xy is any of the rr, rm, etc., triads). In other words, the relative intensities of the pentad peaks should be in the same ratio as those of the triads: 0.12:0.23:0.23:0.42 = 1:1.9:1.9:3.5. Only the rr and rm triads are split into four peaks as expected. The mm triad at δ 6.98 is split into three peaks with relative peak heights of 1:1.8:1.8. (Peak heights are used because the lack of resolution did not permit accurate integration.) If the peak with relative height 1.0 is assigned to the rmmm (or mmmr) pentad, the middle peak to overlapping rmmr and mmmr (or rmmm) peaks, and the remaining peak to the mmmm pentad, the expected intensity ratios are 1:1.5:1.8. If the observed triad ratios are used in place of those calculated from p_m, the expected intensity ratios are 1:1.5:1.6.

The splitting into two nearly equal intensity peaks seen for the mr triad resonance at δ 7.01 can be explained by assigning one of the peaks to an overlap of the mmrr and rmrm pentad resonances and the other to the overlap of the rmrr and mmrm signals. In this case, the expected intensity ratios are 1:1.2 (using the p_m values) or 1:1.0 (using the observed triad ratios). Given the lack of resolution, these fits are acceptable.

The two sets of four peaks centered at δ 7.05 and δ 7.03 should be the easiest to explain, but the intensities of these peaks do not have the expected ratios of 1:2:2:3.5. The δ 7.03 peaks have relative heights of 1:2.3:2.4:1.4 (high field to low), and the δ 7.05 peaks have relative heights of approximately 1:2.0:1.8:1. A possible explanation for the anomalous ratios follows from the fact that, in each cluster of peaks, three of the four peaks have ratios close to the expected 1:2:2, while the fourth peak, corresponding to the rmmr and rmmm pentads, has lower than expected intensity. This could occur if the rmmr and rmmm pentad resonances are sensitive to the heptad structure and are further split into four other partially resolved peaks, thus decreasing the intensity by spreading out the signal. The small peaks in between the main peaks may, in fact, be due to these heptad splittings, but there are insufficient data to warrant further analysis of these peaks at this time.

Another example, that of a P3BT prepared by the Ni(COD)$_2$ coupling of 2,5-dibromo-3-butylthiophene and fractionated by adding chloroform solutions of the polymer to methanol,[20] shows the generality of the statistical approach taken here. This polymer had two α-CH_2 resonances at δ 2.76 and δ 2.53 with relative areas of 0.34 (HT) = p_m and 0.66 (HH) = p_r. At 300 MHz, the ring proton resonances were not sufficiently resolved to permit accurate integration, but the peak positions and relative peak heights are δ 7.04 (0.35), δ 7.01 (0.26), δ 6.99 (0.26), and δ 6.96 (0.13). The relative concentrations of the four triads calculated with $p_m = 0.34$ are 0.44, 0.22, 0.22, and 0.12. Again, the agreement is very good, given the lack of resolution and the use of peak heights instead of peak areas.

Table 1. Number-Average Sequence Length, n_m, and Relative Fractional Concentrations of Sequence Lengths, (m_n), as a Function of the Fractional HT Content, *F* (Absolute Fractional Concentrations Are Obtained by Multiplying Relative Values by p_r^2; See Text)

F =	0.5	0.65	0.75	0.95	0.98
n_m =	2.00	2.86	4.00	20.00	50.00
n\(m_n)					
1	0.50	0.65	0.75	0.95	0.98
2	0.25	0.42	0.56	0.90	0.96
3	0.13	0.27	0.42	0.86	0.94
4	0.06	0.18	0.32	0.81	0.92
5	0.03	0.12	0.24	0.77	0.90
6	0.02	0.08	0.18	0.74	0.89
7	0.01	0.05	0.13	0.70	0.87
8	0.00	0.03	0.10	0.66	0.85
9	0.00	0.02	0.08	0.63	0.83
10	0.00	0.01	0.06	0.60	0.82
11	0.00	0.01	0.04	0.57	0.80
12	0.00	0.01	0.03	0.54	0.78
13	0.00	0.00	0.02	0.51	0.77
14	0.00	0.00	0.02	0.49	0.75
15	0.00	0.00	0.01	0.46	0.74
16	0.00	0.00	0.01	0.44	0.72
17	0.00	0.00	0.01	0.42	0.71
18	0.00	0.00	0.01	0.40	0.70
19	0.00	0.00	0.00	0.38	0.68
20	0.00	0.00	0.00	0.36	0.67
$\sum(n = 1-20)$	1.00	1.86	2.99	12.19	16.29

The above analysis of the NMR spectra of **P3AT**s shows that the HT distribution of diads in these polymers follows "skewed Bernoulian" statistics, as expected for coupling reactions in which there is no site selectivity; i.e., the sequence length distributions (SLDs) are governed by chain end control, as might be expected in a condensation polymerization.[14] The polymer microstructure is completely determined by the single parameter, p_m, given by the HT diad concentration. The number-average sequence length of HT (m) diads, $\bar{n}_m$, is given by $(1 - p_m)^{-1}$. As shown by the values in Table 1, $\bar{n}_m$ increases dramatically as the HT content increases. In the 75% HT polymer, $\bar{n}_m = 4.0$, which rises to 20 and 50 in the 95% and 98% HT polymers, respectively.

Of perhaps more interest than $\bar{n}_m$ is the distribution of HT sequence lengths as a function of HT content. It is widely believed that HH linkages cause the polymer backbone to adopt twisted, nonplanar conformations that disrupt the conjugation between adjacent rings in the HH diad. (The overlap between the p-orbitals on adjacent rings scales as the cosine of the twist angle.) Thus, sequences, e.g., rm_nr, are important in setting the distributions of conjugation lengths as measured, for example, by the UV−vis spectra of conjugated polymers. The fractional concentrations of the rm_nr sequences are given by $p_m^n p_r^2$. Since the factor p_r^2 is common to all these sequence length concentrations, the factor p_r^2 has been dropped from the values shown in Table 1 in order to make relative comparisons easier. Note: as the HT content increases, $p_r \rightarrow 0$, and the concentrations of the (rm_nr) sequences drops as p_r^2. The sum over n of all rm_nr sequences is equal to the concentration of (mr) triads. In addition, Table 1 lists the values of $p_m^n = (m_n)$ for $n = 1-10$. These values represent the *relative* concentration of HT runs, and these relative values are plotted in Figure 5. Also listed in Table 1 are the sums of the fractional concentrations from (m_1) to (m_{10}) (the sum over all sequence lengths, n, of (m_n) converges to $p_m/(1 - p_m) = (m)/(r)$).

Poly(thiophene)s with high HT content are often thought of as being more "homogeneous" than their

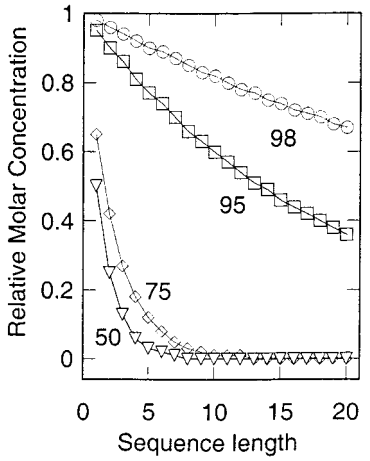

Figure 5. Relative sequence length distributions for HT-polymers with $p_m = 0.5$, 0.75, 0.95, and 0.98.

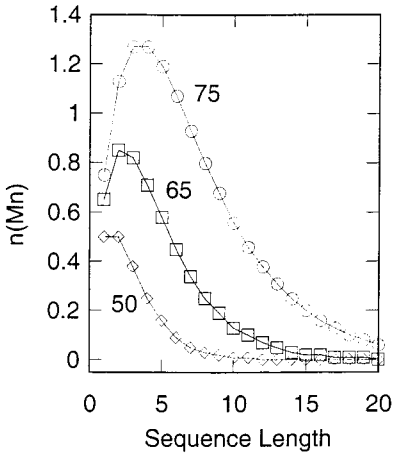

Figure 6. Weighted sequence length distributions for $p_m = 0.5$, 0.65, and 0.75.

counterparts with low HT content.[21] The data in Table 1 and Figure 5 show that, contrary to this popular notion, **P3AT**s with high HT content are actually more heterogeneous in terms of their SLDs and, hence, conjugation lengths than more regiorandom polymers. Thus, in a regiorandom polymer ($p_m = 0.5$), virtually the entire polymer is composed of short runs of HT sequences (m_n with $n \leq 5$). In contrast, the HT SLD for polymers with high HT content is very flat; i.e., the dispersity of the effective conjugation lengths is high. Certain spectral properties, e.g., UV−vis (see below), may depend more on a weighted SLD, $n(m_n)$, rather than on (m_n). Figures 6 and 7 show the number-weighted SLDs for polymers with HT contents of 0.5, 0.65, 0.75, 0.95, and 0.98. Polymers with lower HT content have a peak in the weighted SLD at sequence lengths ≤5, whereas the peak moves out to $n = 20$ and 49 for polymers with HT contents of 95% and 98%, respectively.

Simulation of UV−vis Spectral Line Shapes

The SLDs derived in this work are useful in the interpretation of the line shapes of the $\pi \rightarrow \pi^*$ transitions of **P3AT**s and related polymers as a function of the HT content. If a HH coupling contributes to the disruption of the effective conjugation length by introducing noncoplanarity of adjacent rings, then those polymers with very flat sequence distributions have a correspondingly broad distribution of effective conjugation lengths. The polymers with lower HT content have not only a much shorter average conjugation length but also a narrower distribution of conjugation lengths. We now show how these distributions of effective conjugation lengths affect the profiles of the UV−vis absorption as a function of the HT content of the polymer.

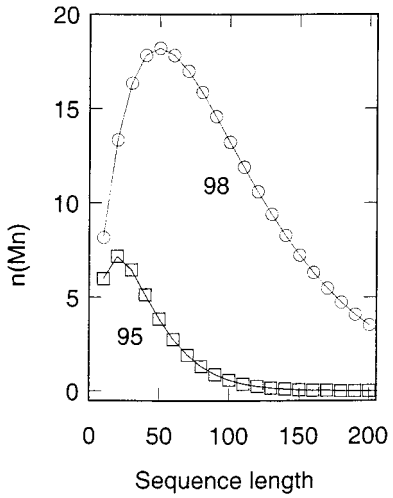

Figure 7. Weighted sequence length distributions for $p_m = 0.95$ and 0.98.

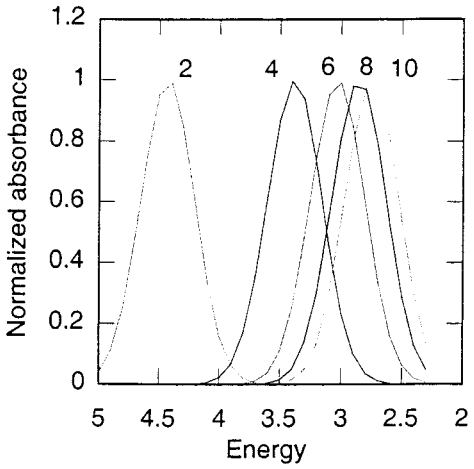

Figure 8. Simulated absorption spectra typical of conjugated oligomers.

It is well-known that the energies of the $\pi \rightarrow \pi^*$ transitions of conjugated heterocyclic or phenylene oligomers are proportional to the reciprocal of the number of rings in the oligomer as illustrated in Figure 8.[10a,22] The peak shapes in Figure 8 are given by the Gaussian, $\rho_n(E) = \exp[-10(E - E_0)]$ (fwhm = 0.53 eV) and E_0 (eV) = 2.33 + 4.22/x, where x is the number of rings in a conjugated sequence. This energy dependence on x is typical for polymers of the type discussed here and results in widely separated peaks for small x that become more closely spaced as the conjugation length increases. Thus, the spectrum of a mixture that is composed primarily of chains with short conjugation lengths is the sum of widely spaced peaks and will appear to be broad. The spectrum of a mixture that contains many conjugation lengths, from short to very long in comparable proportions, will have a relatively narrow peak at low energy because many low-energy peaks, all with nearly the same λ_{max}, are piled on top of one another. Furthermore, the oscillator strengths of oligomers are proportional to the number of rings

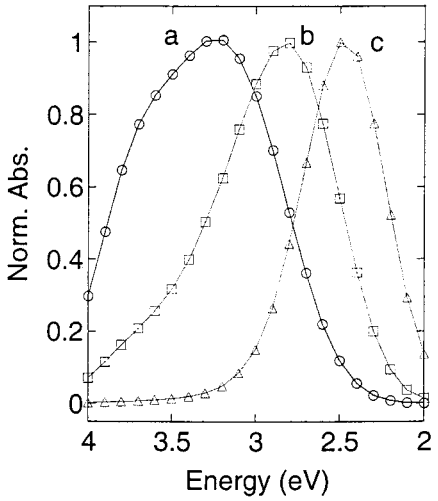

Figure 9. Simulated spectra of polymers with various HT diad contents.

(chromophores) in the conjugated chain. The relationship

$$f(n) = {}^1/_2 n + 0.2 \tag{5}$$

($n = x - 1$; x is the number of rings in the oligomer, and f is the oscillator strength) has been established for a series of bithiazole oligomers.[23] Therefore, the $\pi-\pi^*$ peak profile is given by

$$I(E) = \sum f(n)(\mathrm{m}_n)\rho_n(E) \tag{6}$$

For large n, the weighted distribution $f(n)(\mathrm{m}_n)$ approaches the weighted SLD discussed above and is more appropriate to describe the distribution of peak intensities within the overall peak profile. Figure 9 shows simulated spectra for polymers with 50, 75, and 95% HT contents. These spectra were computed by assuming a HH diad only partially disrupts the conjugation so that E_0 was set as $E_0 = 2.33 + 4.22/(n + 2)$, where $n = (x - 1)$ = number of HT diads in the run, m_n. The absorption corresponding to a given n was weighted with $f(n)$ function described in eq 5, and the final peak profile was the sum over the (m_n) distributions associated with the given HT fraction as described by eq 6.

The simulated spectra show some interesting features. The λ_{max} (nm) and the fwhm (full width at half-maximum, eV) for the simulated spectra in Figure 9, corresponding to the HT contents of 50, 75, and 95% are 380(1.10), 443(0.84), and 498(0.57). That is, the λ_{max} increases with increasing HT content, and the peak width decreases, as seen experimentally (cf. Figure 10). The 95% HT polymer has the narrowest peak even though it is the most heterogeneous in terms of sequence length distribution. This peak profile has a steeply rising low-energy edge, and the presence of the shorter conjugation lengths is revealed by the high-energy "tail" on the peak. The details of the peak shape and fwhm depend on the parameters used in the simulation, especially the weighting function, $f(n)$, the separation between the high- and low-energy limits of the oligomer/polymer absorptions, and individual peak shapes, $\rho_n(E)$. The high-energy "tail" on the 75% and 95% HT polymers becomes more pronounced as the oscillator strength weighting factor of the (m_n) distribution is decreased, and the spectra of the low HT content polymers broaden and even become bimodal as the ratio of b/a increases, where a and b describe the dependence of E_0 on conjugation length, $E_0 = a + b/x$.

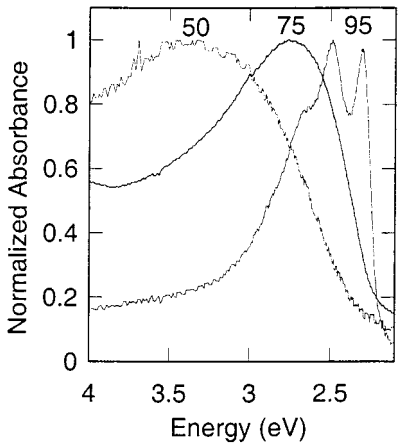

Figure 10. Observed absorption spectra of **P3OF** with HT contents of 50, 75, and 95% (adapted from Figure 6 of ref 9).

Figure 10 shows the experimental spectra of three poly(3-octylfuran)s (**P3OF**) with the three HT contents as indicated. The peak profile of the 95% HT **P3OF** shows the steeply rising low-energy edge and the high-energy tail as simulated using the calculated SLDs. The origins of the fine structure on this peak has been discussed elsewhere,[1a,9] and no attempt was made to model it in this work. The absorption peaks of the 50% and 75% HT **P3OF**s show the sloping low-energy edge as predicted by the simulation, but the high-energy edges are obscured by further high-energy, $\pi-\pi^*$ and $n-\pi^*$ absorptions, the origins of which will be discussed elsewhere. The fwhm of the peaks are 0.54, 0.84, and ca. 1.38 eV respectively for the polymers with 95, 75, and 50% HT contents. (The last fwhm is probably exaggerated by the overlap of the other $\pi-\pi^*$ and $n-\pi^*$ peaks at higher energies.) Similar data are available for **P3AT**s. Rieke et al. have published spectra of poly(3-hexylthiophenes) with varying amounts of HT content. As measured from the figures in ref 5a, the fwhm of **P3HT** with 50, 65, 70, and 98.5% HT content are 2.00, 1.18, 1.81, and 0.92 eV, respectively. These data show a nonmonotonic change in the peak widths for the polymers with intermediate HT content. This behavior is modeled in the simulated spectra when a smaller weighting factor, $f(n)$, is used, and when there is not a too large separation between the peak energies of the polymers with low and high HT content.

Conclusions

P3ATs and related conjugated polymers are described in terms of HT ("m") and HH ("r") diads in order to delineate the SLDs using the well-known formalisms of vinyl polymer microstructure. Contrary to the usual description, regioregular polymers are more "heterogeneous" in terms of SLDs and, hence, effective conjugation lengths than their less regular counterparts. Despite the heterogeneity, the spectra of regioregular polymers are more narrow than the less disperse polymers with low HT content.

Acknowledgment. The author thanks the National Science Foundation for support of this research through Grant DMR-9986123 and expresses his appreciation to P. G. Rasmussen and M. Dimmic for helpful discussions.

References and Notes

(1) (a) Koren, A. B.; Curtis, M. D.; Kampf, J. W. *Chem. Mater.* **2000**, *12*, 1519. (b) Yamamoto, T.; Komarudin, D.; Arai, M.; Lee, B.; Suganuma, H.; Asakawa, N.; Inoue, Y.; Kubota, K.; Sasaki, S.; Fukuda, T.; Matsuda, H. *J. Am. Chem. Soc.* **1998**, *120*, 2047. (c) Halkyard, C. E.; Rampey, M. E.; Kloppenburg, L.; Studer-Martinez, S. L.; Bunz, U. H. F. *Macromolecules* **1998**, *31*, 8655. (d) (a) Langeveld-Voss, B. M. W.; Janssen, R. A. J.; Christiaans, M. P. T.; Meskers, S. C. J.; Dekkers, H. P. J. M.; Meijer, E. W. *J. Am. Chem. Soc.* **1996**, *118*, 4908. (e) Langeveld-Voss, B. M. W.; Waterval, R. J. M.; Janssen, R. A. J.; Meijer, E. W. *Macromolecules* **1999**, *32*, 227. (f) Dimitrakapoulos, C. D.; Mascaro, D. J. *IBM J. Res. Dev.* **2001**, *45*, 11.

(2) (a) Yamamoto, T.; Maruyama, T.; Zhou, Z.; Ito, T.; Fukuda, T.; Yoneda, Y.; Gegum, F.; Ikeda, T. S.; Tahezoe, H.; Fukuda, A.; Kubota, K. *J. Am. Chem. Soc.* **1994**, *116*, 4832. (b) Grem, G.; Paar, C.; Stmpfl, J.; Leising, G.; Huber, J.; Scherf, U. *Chem. Mater.* **1995**, *7*, 2. (c) Li, H.; Powell, D. R.; Hayanashi, R. K.; West, R. *Macromolecules* **1998**, *31*, 52. (d) Xu, B.; Holdcroft, S. *Macromolecules* **1993**, *26*, 4457.

(3) (a) Bunz, U. H. F.; Enkelmann, V.; Kloppenburg, L.; Jones, D.; Shimizu, K. D.; Claridge, J. B.; zur Loye, H.; Leiser, G. *Chem. Mater.* **1999**, *11*, 1416. (b) Halkyard, C. E.; Rampey, M. E.; Kloppenburg, L.; Studer-Martinez, S. L.; Bunz, U. H. F. *Macromolecules* **1998**, *31*, 8655.

(4) (a) McCullough, R. D.; Tristram-Nagle, S.; Williams, S. P.; Lowe, R. D.; Jayaraman, M. *J. Am. Chem. Soc.* **1993**, *115*, 4910. (b) McCullough, R. D.; Williams, S. P. *J. Am. Chem. Soc.* **1993**, *115*, 11608.

(5) (a) Chen, T.; Wu, X.; Rieke, R. D. *J. Am. Chem. Soc.* **1995**, *117*, 233. (b) Wu, X.; Chen, T.; Rieke, R. D. *Macromolecules* **1996**, *29*, 7671. (c) Faid, K.; Frechette, M.; Ranger, M.; Mazerolle, L.; Levesque, I.; Leclerc, M.; Chen, T.; Rieke, R. D. *Chem. Mater.* **1995**, *7*, 1390. (d) Sandstedt, C. A.; Rieke, R. D.; Eckhardt, C. J. *Chem. Mater.* **1995**, *7*, 1057. (e) Chen, T.; Rieke, R. D. *J. Am. Chem. Soc.* **1992**, *114*, 10087.

(6) (a) Hong, Y.; Miller, L. L. *Chem. Mater.* **1995**, *7*, 1999. (b) Duan, R. G.; Miller, L. L.; Tomalia, D. A. *J. Am. Chem. Soc.* **1995**, *117*, 10783. (c) Bach, C. M.; Reynolds, J. R. *J. Phys. Chem.* **1994**, *98*, 13636. (d) Sato, M.; Hiroi, M. *Synth. Met.* **1995**, *69*, 307. (d) Hill, M. G.; Penneau, J. F.; Zinger, B.; Mann, K. R.; Miller, L. L. *Chem. Mater.* **1992**, *4*, 1106. (e) Graf, D. D.; Duan, R. G.; Campbel, J. P.; Miller, L. L.; Mann, K. R. *J. Am. Chem. Soc.* **1997**, *119*, 5888. (f) Boden, N.; Borner, R. C.; Bushby, R. J.; Clements, J. *J. Am. Chem. Soc.* **1994**, *116*, 10807. (g) Miller, L. L.; Zhong, C.; Kasal, P. *J. Am. Chem. Soc.* **1993**, *115*, 5982.

(7) (a) Torsi, L.; Dodabalapur, A.; Lovinger, A. J.; Katz, H. E.; Ruel, R.; Davis, D. D.; Baldwin, K. W. *Chem. Mater.* **1995**, *7*, 2247. (b) Lovinger, A. J.; Rothberg, L. J. *J. Mater. Res.* **1996**, *11*, 1581. (c) Torsi, L.; Dodabalapur, A.; Rothberg, L. J.; Fung, A, W. P.; Katz, H. E. *Science* **1996**, *272*, 1462.

(8) (a) Yang, C.; Orfino, F. P.; Holdcroft, S. *Macromolecules* **1996**, *29*, 6510. (b) Park, K. C.; Levon, K. *Macromolecules* **1997**, *30*, 3175. (c) Prosa, T. J.; Winokur, M. J.; McCullough, R. D. *Macromolecules* **1996**, *29*, 3654.

(9) Politis, J. K.; Nemes, J. C.; Curtis, M. D. *J. Am. Chem. Soc.* **2001**, *123*, 2537.

(10) (a) Nanos, J. I.; Kampf, J. W.; Curtis, M. D.; Gonzalez, L.; Martin, D. C. *Chem. Mater.* **1995**, *7*, 2232. (b) Gonzales Ronda, L.; Martin, D. C.; Nanos, J. I.; Politis, J. K.; Curtis, M. D. *Macromolecules* **1999**, *32*, 4558.

(11) (a) Politis, J. K.; Curtis, M. D.; González-Ronda, L.; Martin, D. C. *Chem. Mater.* **2000**, *12*, 2798. (b) Politis, J. K.; Somaoza, F. B.; Kampf, J. W.; Curtis, M. D.; González-Ronda, L.; Martin, D. C. *Chem. Mater.* **1999**, *11*, 2274.

(12) (a) Haba, O.; Hayakawa, T.; Ueda, M.; Kawaguchi, H.; Kawazoe, T. *React. Funct. Polym.* **1998**, *37*, 163. (b) Andersson, M. R.; Mammo, W.; Olinga, T.; Svensson, M.; Theander, M.; Inganäs, O. *Synth. Met.* **1999**, *101*, 11. (c) Amou, S.; Haba, O.; Shirato, K.; Hayakawa, T.; Ueda, M.; Takeuchi, K.; Asai, M. *J. Polym. Sci., Part A: Polym. Chem.* **1999**, *37*, 1943. (d) Miyasaka, M.; Yamazaki, T.; Tsuchida, E.; Nishide, H. *Macromolecules* **2000**, *33*, 8211. (e) Frechette, M.; Belletête, M.; Bergeron, J.-Y.; Durocher, G.; Leclerc, M. *Synth. Met.* **1997**, *84*, 11.

(13) Price, F. P. In *Markov Chains and Monte Carlo Calculations in Polymer Science*; Lowry, C. G., Ed.; Dekker: New York, 1970.

(14) (a) Farina, M.; DiSilvestro, Ferragni, A. *Macromol. Chem. Phys.* **1995**, *196*, 353. (b) Busico, V.; Cipullo, R. *Prog. Polym. Sci.* **2001**, *26*, 443.

(15) (a) Bovey, F. A. *Polymer Conformation and Configuration*; Academic Press: New York, 1969. (b) Bovey, F. A. *Acc. Chem. Res.* **1968**, *1*, 175.

(16) Randall, J. C. *Polymer Sequence Determination-Carbon-13 NMR Method*; Academic Press: New York, 1977.

(17) (a) Curtis, M. D.; McClain, M. D. *Chem. Mater.* **1996**, *8*, 936. (b) McClain, M. D. Ph.D. Thesis, The University of Michigan, 1994; p 48.

(18) Barbarella, G.; Bongini, A.; Zambianchi, M. *Macromolecules* **1994**, *27*, 3039.

(19) (a) Sato, M.; Morii, H. *Polym. Commun.* **1991**, *32*, 42. (b) Sato, M.; Morii, H. *Macromolecules* **1991**, *24*, 1196.

(20) The author thanks Mr. Li Tan, University of Michigan, for sharing these data.

(21) Louarn, G.; Trznadel, M.; Buisson, J. P.; Laska, J.; Pron, A.; Lapkowski, M.; Lefrant, S. *J. Phys. Chem.* **1996**, *100*, 12532.

(22) Bidan, G.; De Nicola, A.; Enée, V.; Guillerez, S. *Chem. Mater.* **1998**, *10*, 1052.

(23) Blanda, W. M. Ph.D. Thesis, The University of Michigan, 2000; pp 197.

MA011053J